Bandwidth Extension of Planar Antennas Using Embedded Slits for Reliable Multiband RF Communications

Mohammad Alibakhshi-Kenari, Mohammad Naser-Moghadasi, R.A. Sadeghzadeh, Bal S. Virdee, Ernesto Limiti

PII: S1434-8411(16)30111-X
DOI: http://dx.doi.org/10.1016/j.aeue.2016.04.003
Reference: AEUE 51601

To appear in: *AEUE - International Journal of Electronics and Communications*

Received Date: 10 January 2016
Accepted Date: 2 April 2016

Please cite this article as: M. Alibakhshi-Kenari, M. Naser-Moghadasi, R.A. Sadeghzadeh, B.S. Virdee, E. Limiti, Bandwidth Extension of Planar Antennas Using Embedded Slits for Reliable Multiband RF Communications, *AEUE - International Journal of Electronics and Communications* (2016), doi: http://dx.doi.org/10.1016/j.aeue.2016.04.003

Bandwidth Extension of Planar Antennas Using Embedded Slits for Reliable Multiband RF Communications

Mohammad Alibakhshi-Kenari[1]*, Mohammad Naser-Moghadasi[1], R. A. Sadeghzadeh[2], Bal S. Virdee[3] and Ernesto Limiti[4]
[1] Faculty of Eng., Science and Research Branch, Islamic Azad University, Tehran- IRAN
[2] Faculty of Electrical and Computer Eng., K. N. University of Technology, Tehran- IRAN
[3] London Metropolitan University, Center for Communications Technology, Faculty of Life Sciences and Computing, London N7 8DB, UK
[4]Dipartimento di Ingegneria Elettronica, Università degli Studi di Roma Tor Vergata, Via del Politecnico 1, 00133 Roma – ITALY

makenari@mtu.edu[1]*, mn.moghaddasi@srbiau.ac.ir[1], sadeghz@eetd.kntu.ac.ir[2], b.virdee@londonmet.ac.uk[3], and limiti@ing.uniroma2.it[4]

Abstract — **In this paper a technique is described to extend the impedance bandwidth of patch antennas without compromising their size. This is accomplished by embedding capacitive slits in the rectangular patch with a truncated ground-plane, and exciting the antenna through a meandered strip-line feed. The proposed antenna was fabricated on standard FR-4 substrate with permittivity of 4.6, thickness of 0.8 mm and loss-tangent of 0.001. The performance of the prototype antenna was verified through measurements. Characteristics of the antenna include an impedance bandwidth of 5.25 GHz (800 MHz–6.05 GHz) for VSWR<2 corresponding to a fractional bandwidth of 153.28%, peak gain of 5.35 dBi, radiation efficiency of 84.12% at 4.45 GHz, and low cross-polarization. These attributes make the antenna applicable for stable and reliable multiband applications in the UHF, L, S and major part of C-bands. The antenna offers advantages of low cost, low profile, ease of manufacturing, durability and conformability.**

Index Terms — **Planar slit antenna, meandered strip-line feed, wideband antenna, multiband antenna.**

I. INTRODUCTION

Antennas are essential components in wireless communications but whose size and operational frequency bandwidth can be limiting factors. Hence the next generation wireless systems demand stringent requirements from antennas, in particular, characteristics including multiband operation, light-weight, low profile, cost effectiveness, portability, compactness, efficiency and reliability. Multiband functionality in antennas has become a fundamental requirement to equip wireless devices with multiple communication standards so that they can utilize the crowded electromagnetic spectrum more efficiently and effectively. This is necessary to ensure global portability and enhancing capacity requirements [1]. To meet these requirements microstrip technology offers considerable size reduction and cost effectiveness as antennas can be manufactured easily in mass production. Also such antennas can conform to planar or cylindrical surfaces [2],[3]. However, such antennas suffer from narrow bandwidth. To overcome this deficiency various techniques have been investigated recently, which include: introducing slit-lines [4] in the patch antenna; implementing unusual feeding techniques [5]; incorporating parasitic elements around the radiating patch [6]; taper matching the patch antenna [7]; embedding an array of metallic structures that act as an electromagnetic band-gap (EBG) [8]; employing meta-surface [9],[10]; and loading the antenna with metamaterial

unit-cells [11]. Although these techniques have been shown to increase the impedance bandwidth of microstrip based antennas however the bandwidth enhancement is limited for multiband applications. Recently the idea of using meandered strip-line fed patch antenna to widen the bandwidth of patch antennas has raised some interest among the antenna researchers as this technique is less cumbersome to implement [12].

The antenna proposed in this paper will be developed for RFID and WiMAX systems. The UHF band is extensively used RFID systems for organizational and commercial applications for tracking and identification capabilities. In Europe the UHF RFID system functions over 865–867 MHz, and in North America over 902–928 MHz [13]. On the other hand, WiMAX is based upon IEEE 802.16-2004, which was later modified to IEEE Std. 802.16e-2005 and it has different spectrum allocation in different parts of the world based on the standard band 2.3 GHz, 2.5 GHz and 3.5 GHz [14].

In this paper, a planar monopole antenna with a truncated ground-plane is presented for multiband wireless communications systems. This is achieved by embedding in the antenna's radiating patch an H-shaped and a pair of inverted U-shaped capacitive slits, and exciting the antenna through a meandered strip-line. The antenna was fabricated on commercially available FR-4 substrate with permittivity of 4.6, thickness of 0.8 mm and $\tan\delta = 0.001$. The antenna occupies an area of 13.5×12.7 mm^2 or $0.036\lambda_0 \times 0.033\lambda_0$, where free-space wavelength is 0.8 GHz. The location of the slits in the rectangular patch and the meandered-line feed structure were determined through parametric analysis. The performance of the antenna was verified through measurement. The proposed antenna possesses properties of low-profile, ease of manufacture and integration in RF transceivers, low cost as no via holes are used and low cross-polarization. These characteristics make it suitable for multiband applications such as: UHF RFID, GPS, PCS, DCS, WiMAX, WLAN, WiFi, Bluetooth, and other applications in the UHF, L, S, major part of C-bands.

II. DESIGN PROCEDURE OF A STEPPED IMPEDANCE MONOPOLE ANTENNA

The design technique proposed here offers expansion of the impedance bandwidth of the antenna without compromising its size and salient characteristics. This is achieved by inserting an H-shaped slit in the radiating patch and exciting the antenna using a meandered strip-line. The antenna structure excludes the use of via-holes to avoid unnecessary complexity and manufacturing cost. Two different slit structures, i.e. H-shape and inverted U-shape, were employed in the antenna design. Cutout in the patch of the Antenna#1 was an H-shaped slit. In Antenna#2 and #3 an inverted U-shaped slit is cutout on the left and right hand side, respectively, of the H-shape slit. In the final antenna, Antenna#4, the inverted U-shaped slits were located on either sides of the H-shape slit. By comparing the characteristics of these antennas reveals the Antenna#4 exhibits a much better performance. The effect of the meandered strip-line feed was investigated using ANSYS HFSS 3-D full-wave electromagnetic fields simulation tool [15]. The optimization of feeding line dimensions has resulted in impedance bandwidth broadening of the antenna.

A. Patch antenna with H-shaped slit

The generic patch antenna configuration is shown in Fig. 1(a) and (b). The equivalent circuit model of the antenna in Fig. 1(c) shows it is constituted from composite right/left-handed transmission-line (CRLH-TL). The H-shaped slit essentially behaves as series capacitors (C_L), and high impedance meandered strip-line feed-line is

represented by inductor (L_L). Other losses introduced by the antenna structure are represented by series right-handed resistance (R_R), shunt left-handed resistance (R_L), series conductance (G_L) and shunt conductance (G_R).

Location and dimensions of the slit were optimized using ANSYS HFSS simulator. The slit is located in center of patch in order to concentrate the electromagnetic fields and currents near the antenna structure to effectively prevent the fields from spreading along the antenna's ground-plane which would otherwise contribute towards unwanted coupling. This technique of embedding a slit allows the implementation of a smaller sized antenna, and such a structure in an array minimizes mutual coupling which is important to de-correlate multipath channels in small cellular systems. The meandered strip-line feed is used here to increase the impedance bandwidth and suppress cross-polarization as reported in [12]. It also helps to eliminate unwanted notch bands in the antenna's response due to impedance mismatch, thus providing bandwidth extension.

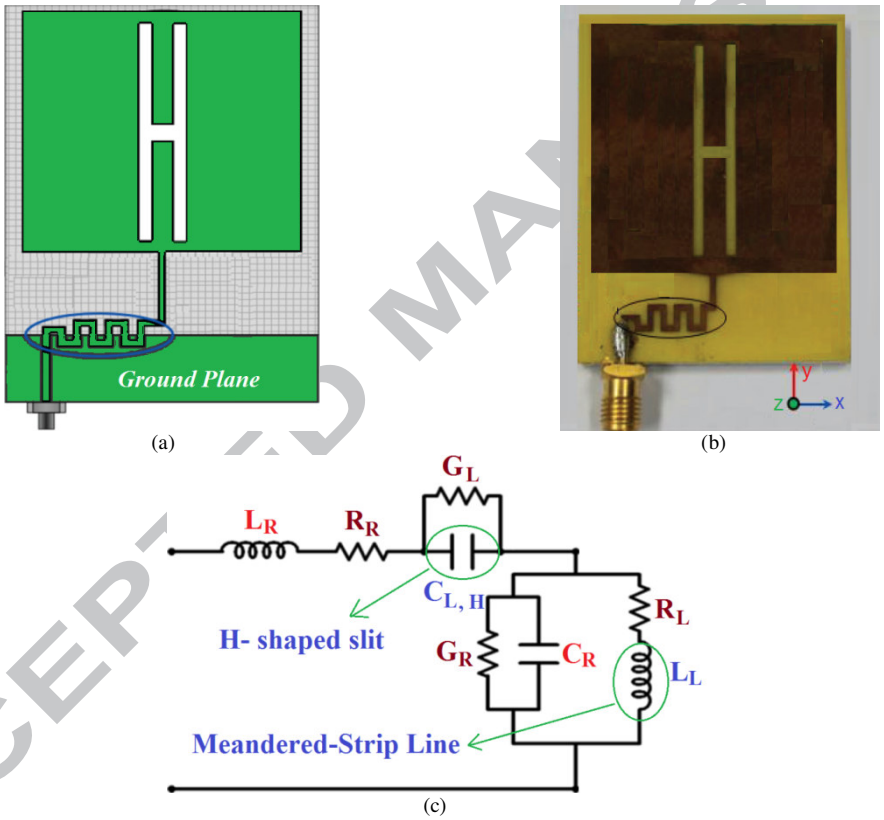

Fig. 1. Antenna#1 patch includes an H-shaped slit and is excited through a meandered strip-line feed, (a) simulation model, (b) fabricated prototype, and (c) equivalent circuit model.

Length (L), width (W) and height (h) of the proposed antenna are 21.2 mm, 15 mm and 0.8 mm, respectively. The length (L_p) and width (W_p) of radiation patch are 13.5 mm and 12.7 mm, respectively. The corresponding electrical size of the antenna and radiation patch is $0.155\lambda_0 \times 0.110\lambda_0 \times 0.005\lambda_0$ and $0.099\lambda_0 \times 0.093\lambda_0$, respectively, where λ_0 is free-space wavelength at 2.2 GHz. The simulated and measured reflection-coefficient of the antenna are shown in Fig. 2(a). The simulated impedance bandwidth of the antenna for S_{11}<-10 dB is 2.58 GHz (2.05–4.63 GHz), which corresponds to a fractional bandwidth of 77.24%. The antenna has a measured bandwidth of 2.3 GHz

(2.2–4.5 GHz), which corresponds to fractional bandwidth of 68.65%. In the simulated response the antenna resonates at $f_{r,simulated}$ =3.62 GHz, and in the measured response at $f_{r,measured}$ =3.55 GHz. The discrepancy in bandwidth is attributed to manufacturing tolerance. The antenna has an operational bandwidth of 2.2–4.5 GHz.

The measured gain and radiation efficiency of the antenna is shown in Fig. 2(b). At spot frequencies of 2.2, 3.55 and 4.5 GHz the gain and radiation efficiency are 0.65 dBi and 18.34%, 2.75 dBi and 47.15%, and 1.90 dBi and 36.12%, respectively.

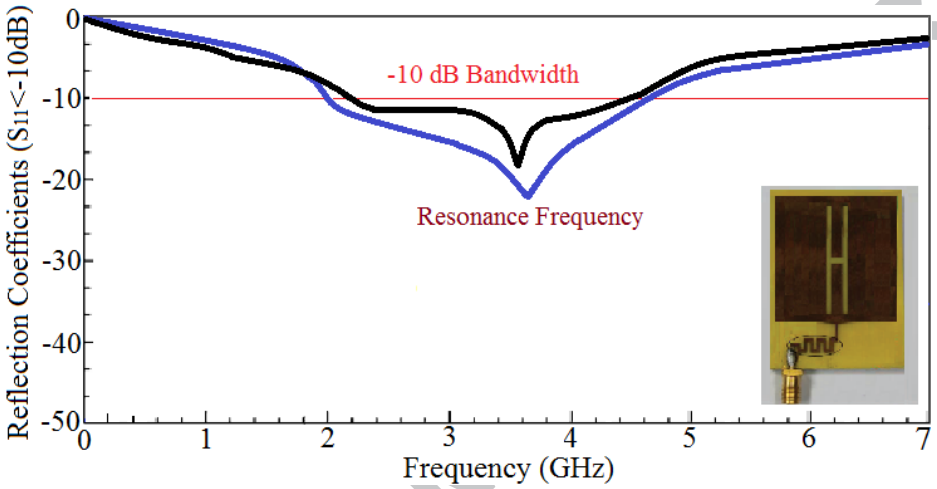

Fig. 2. (a) Simulated (blue line) and measured (black line) reflection-coefficient response of the antenna.

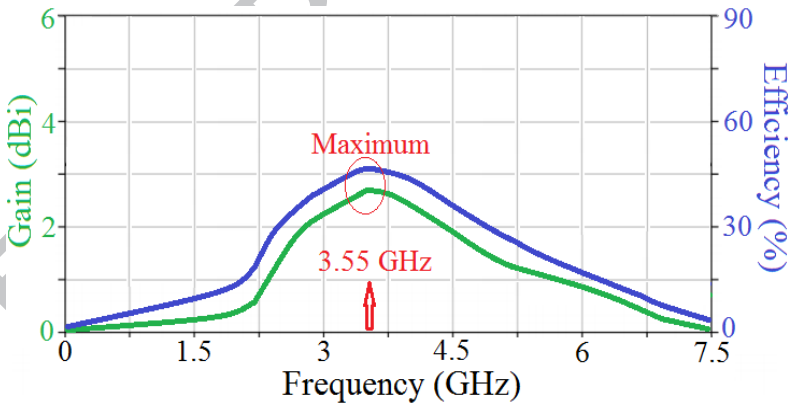

Fig. 2. (b) Measured gain and radiation efficiency response of Antenna#1.

Fig. 3 shows the measured co-polarization and cross-polarization radiation patterns of the antenna in the E(*yz*)- and H(*xz*) planes at its resonance frequency of f_r =3.55 GHz. Measurements shows the antenna radiates omni-directionally in the E-plane and bi-directionally in the H-plane. This antenna has a high cross polarization, which is unacceptable for practical applications. The cross polarization is generated by the H-shaped slit that excites two orthogonal modes in phase quadrature. The cross polarization can be suppressed by inserting U-shaped slits as shown below.

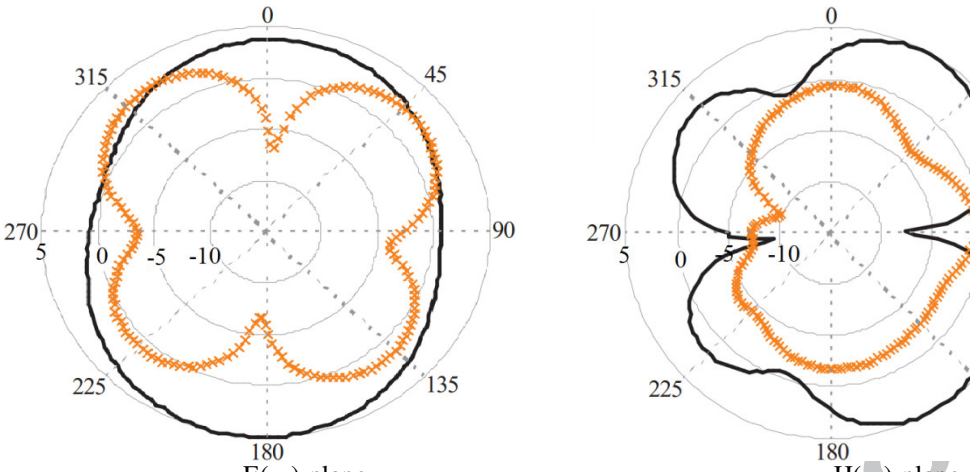

Fig. 3. Measured radiation patterns of Antenna#1 at the resonance frequency of 3.55 GHz. [solid line: co-polarization, and crossed line: cross-polarization].

B. Effect of inverted U-shaped slit located on the left-hand side of the H-shaped slit

In order to improve the performance of the antenna another slit was embedded on the left-hand side to the H-shaped slit, as shown in Fig. 4. The slit resembles an inverted U-shape. The dimensions of the patch and the feed structure were unaltered. The inverted U-shaped slit essentially enhances the series LH capacitance (C_L). The effective area or aperture of the antenna is extended by the slit.

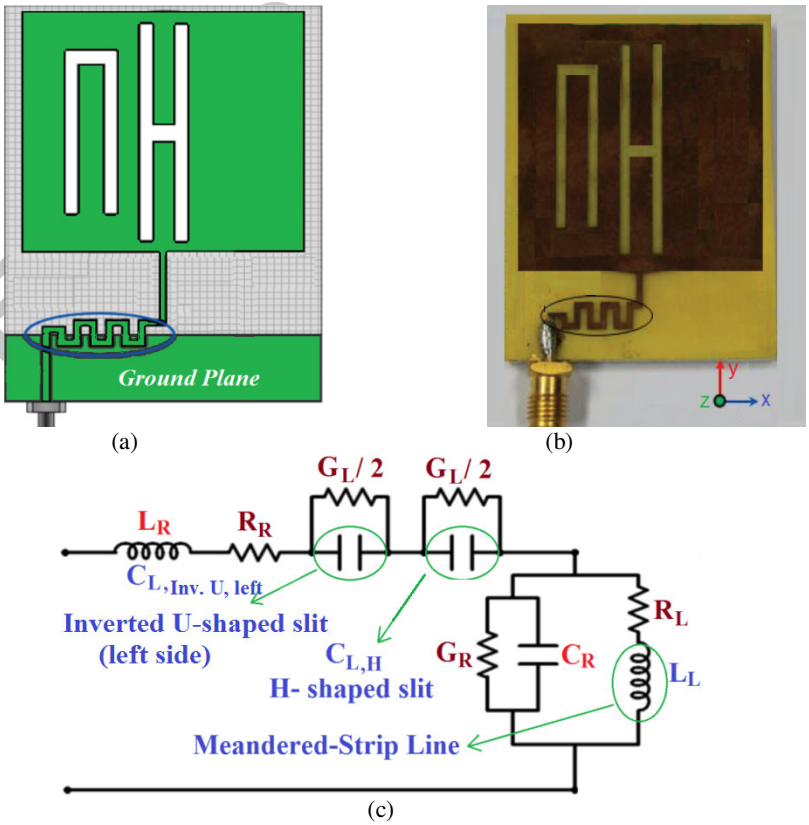

Fig. 4. Configuration of Antenna#2 with inverted U-shaped slit on the left-hand side of the H-shaped slit, (a) HFSS model, (b) fabricated structure, and (c) equivalent circuit model.

Simulation response in Fig. 5(a) shows the resulting impedance bandwidth of the antenna for S_{11}<-10 dB is now 3.8 GHz (0.95–4.75 GHz), which corresponds to a fractional bandwidth of 133.33%. The antenna now resonates at two frequencies f_{r1} =2.2 GHz and f_{r2} =3.6 GHz. The first resonance frequency is due to the inverted U-shaped slit and the second due to the H-shaped slit.

Fig. 5(a) shows the measured response closely agrees with the simulation. The measured impedance bandwidth is 3.55 GHz (1.1–4.65 GHz), which corresponds to a fractional bandwidth of 123.47%. The antenna resonates at 2.25 GHz and 3.45 GHz, making it suitable for WiMAX, WiFi, and Bluetooth systems. The measured gain and radiation efficiency of antenna are shown in Fig. 5(b). At operational frequencies of 1.1, 2.25, 3.45 and 4.65 GHz the gain and radiation efficiency are 0.50 dBi and 15.7%, 3.27 dBi and 58.34%, 4.55 dBi and 72.50%, and 2.10 dBi and 43.12%, respectively. The peak gain and efficiency is observed at the second resonance frequency of 3.45 GHz.

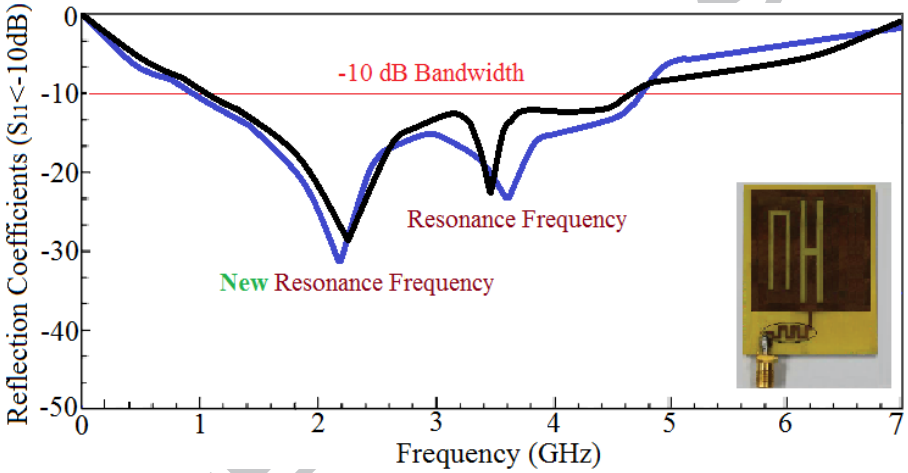

Fig. 5. (a) Simulated (blue line) and measured (black line) reflection-coefficient response of the Antenna#2.

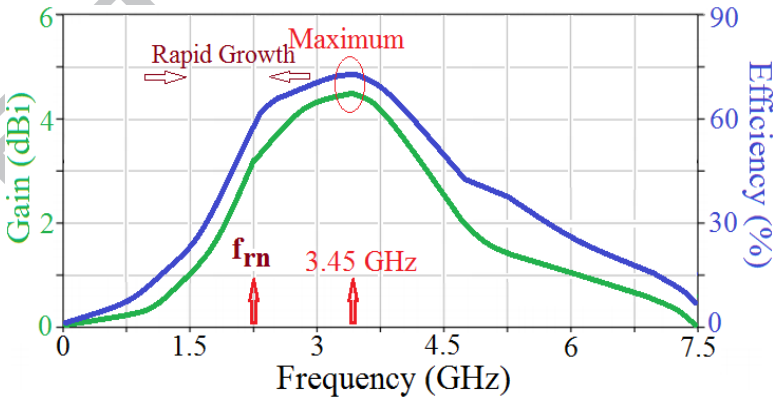

Fig. 5. (b) Measured gain and radiation efficiency of Antenna#2.

The measured radiation patterns of the proposed antenna in E- and H-planes at the two resonance frequencies (2.25 GHz and 3.45 GHz) are shown in Fig. 6. The radiation is omni-directional in the E-plane and bi-directional in the H-plane. Insertion of the U-shaped slit in the patch results in reduction in the cross-polarization compared to Antenna#1.

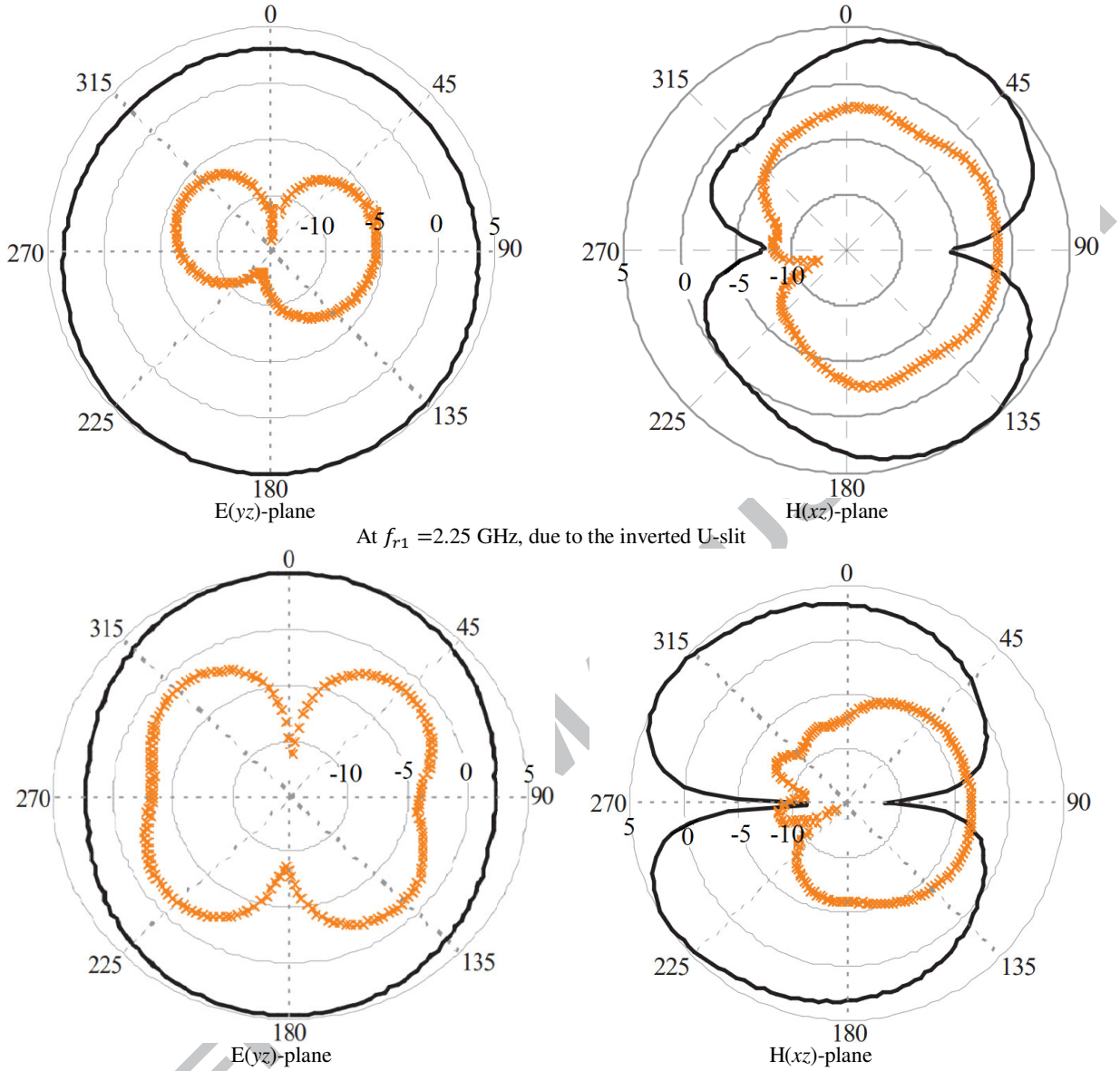

Fig. 6. Measured radiation patterns at the two resonance frequencies. Left column: E(*yz*)-plane pattern; Right column: H (*xz*)-plane pattern of Antenna#2. [Solid line: co-polarization, and crossed line: cross-polarization].

C. Effect of the inverted U-shaped slit located on the right-hand side of the H-shaped slit

The effect on the antenna performance was investigated by locating the inverted U-shape slit on the right-hand side of the H-shape slit, as shown in Fig. 7, without changing the dimensions of the antenna and meandering strip-line feed. The equivalent circuit of Antenna#3 is shown in Fig. 7(c). As mentioned earlier the inverted U-shaped slit essentially behaves like a series left-handed capacitance (C_L), consequently enhancing the overall series capacitance which leads to the extension in the antenna bandwidth.

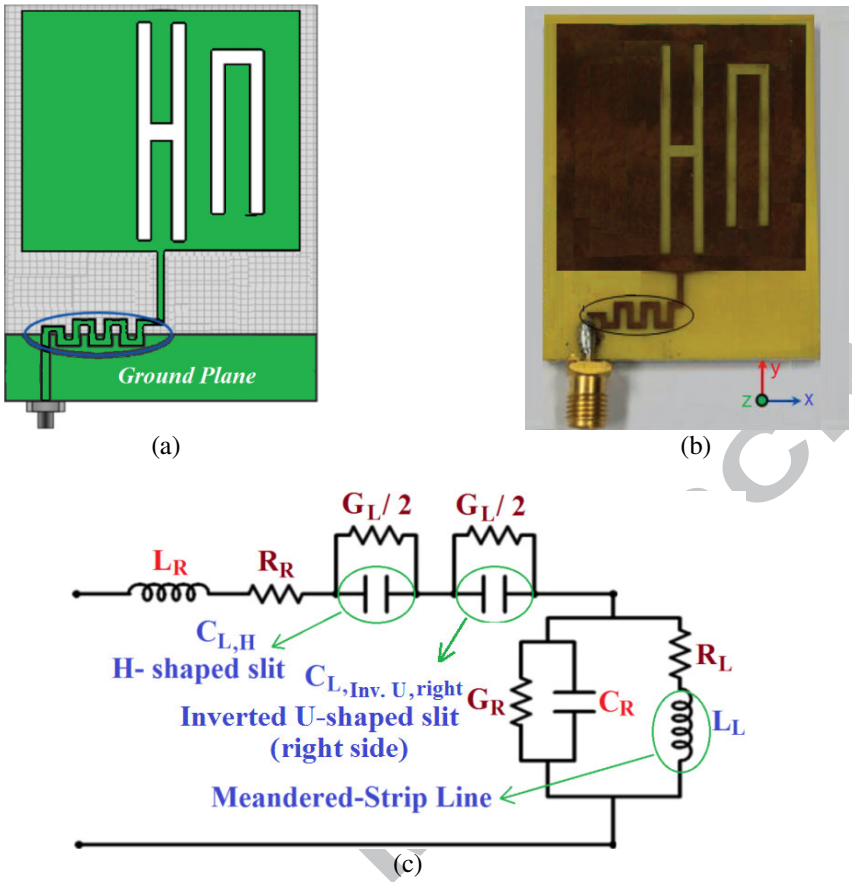

Fig. 7. Layout of Antenna#3 with the inverted U-shaped slit embedded on the right-hand side of the centrally located H-shape slit, (a) simulation model, (b) fabricated layout, and (c) equivalent circuit model.

Fig. 8(a) shows the simulated impedance bandwidth of Antenna#3 is 4.03 GHz (1.85–5.88 GHz) corresponding to a fractional bandwidth of 104.26%. The antenna resonates at 3.45 GHz and 4.55 GHz resulting, respectively, from the H-slit and inverted U-shape slit. Simulation and measured results show the relative location of the U-shaped slit on the patch antenna determines how it interacts with the H-shaped slit. Hence the resonant mode frequency of the U-shaped slit shown in Fig. 8(a) is different from Fig. 5(a). The measured reflection-coefficient in Fig. 8(a) agrees closely with the simulation. The measured impedance bandwidth is 3.75 GHz (2–5.75 GHz), which corresponds to a fractional bandwidth of 96.77%. The fabricated antenna resonates at 3.5 GHz and 4.6 GHz. Antenna#3 operates across 2–5.75 GHz making it suitable for WiMAX, WiFi, Bluetooth and other communication services.

The measured gain and radiation efficiency in Fig. 8(b) at 2, 3.5, 4.6 and 5.75 GHz are 0.75 dBi and 21.50%, 3.05 dBi and 53.76%, 4.70 dBi and 75.18%, and 2.35 dBi and 47.10%, respectively. The optimum gain and radiation efficiency are at 4.6 GHz, which is associated with the resonance frequency of the inverted U-shaped slit.

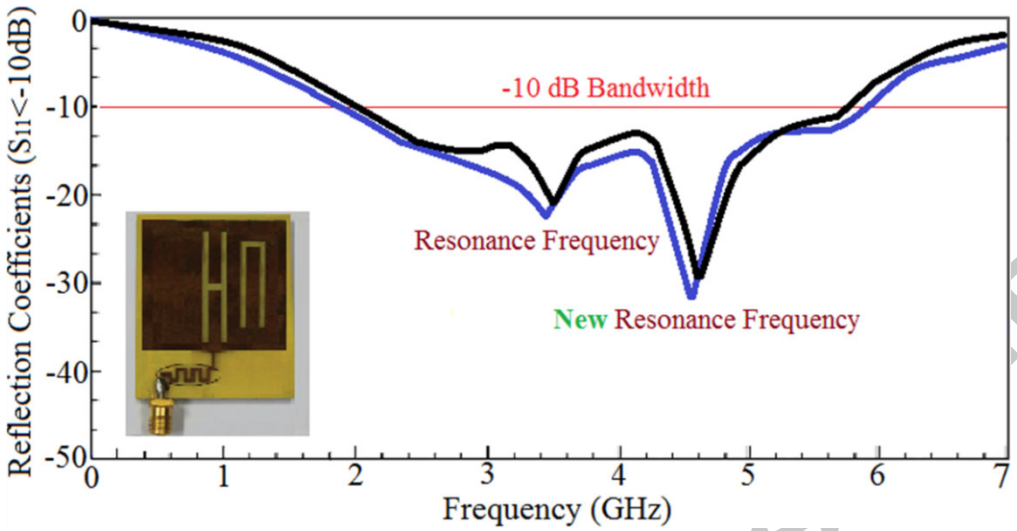

Fig. 8. (a) Simulated (blue line) and measured (black line) reflection-coefficient of Antenna#3.

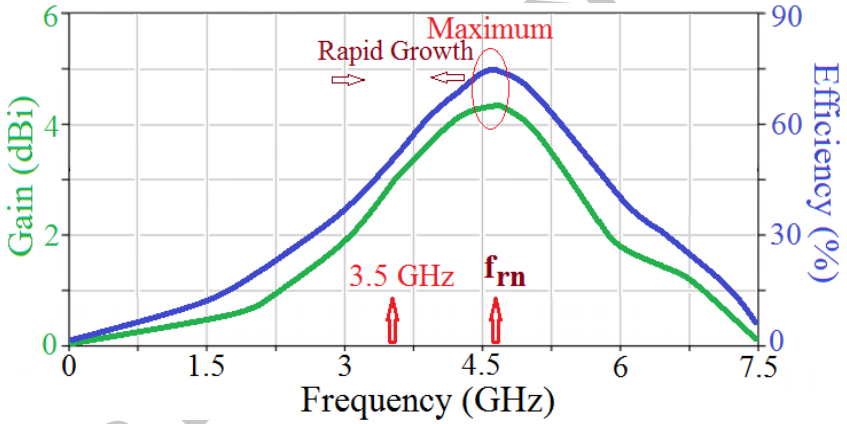

Fig. 8. (b) Measured gain and radiation efficiency of Antenna#3.

The radiation patterns of the proposed antenna in E- and H-planes were measured at its resonance frequencies. The measured co-polarization and cross-polarization radiation patterns at 3.5 GHz and 4.6 GHz in E- and H-planes are shown in Fig. 9. It can be observed that in E-plane the antenna radiates omni-directionally, and in the H-plane it radiates bi-directionally, which is similar to a monopole antenna.

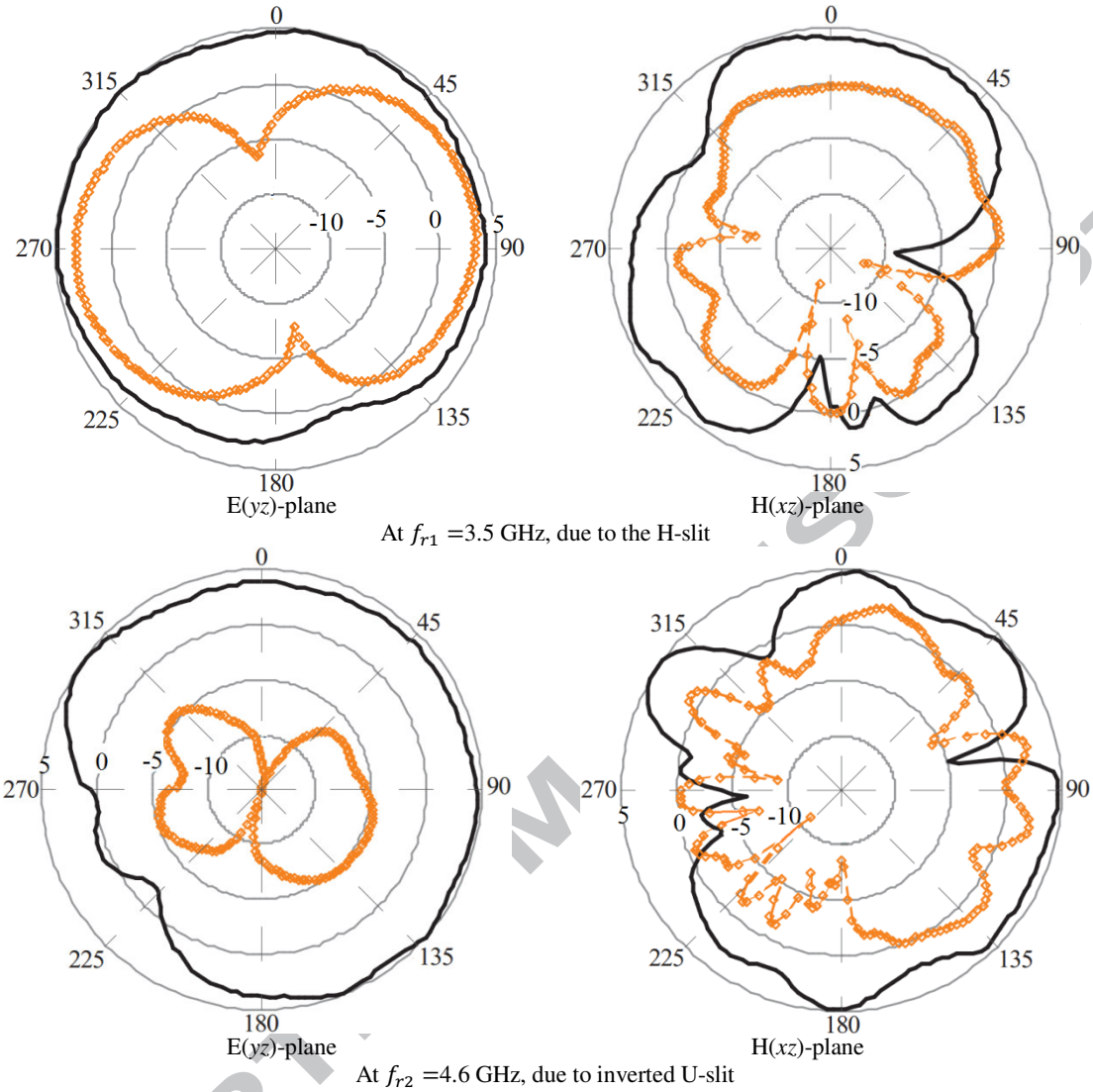

Fig. 9. The measured radiation patterns at 3.5 and 4.6 GHz. [Solid line: co-polarization, and crossed line: cross-polarization].

D. Patch antenna with two inverted U-shape slits located on either of the H-shape slit

Antenna#4 is a combination of Antennas#2 and #3, where two inverted U-shape slits are located on either sides of the main H-shape slit, as shown in Fig. 10. The dimensions of antenna and the meandering strip-line feed are unaltered. The dimensions of the antenna structure are given in Table 1.

The equivalent circuit model of the proposed symmetrical antenna structure in Fig. 10(e) consists of the composite right/left-handed transmission-line, where parasitic series reactance is represented by inductor L_R and shunt capacitor C_R. It is noticeable that, the unavoidable currents that flow on the patch establishes series inductance L_R and the shunt capacitance C_R is mostly come from the gap capacitance between the patch and the ground-plane, which indicates that these inductance and capacitance cannot be ignored. Series resonance is due to L_R and C_L, and shunt resonance due to C_R and L_L. At low frequency, C_L and L_L are dominant so the transmission-line circuit shows the left-handed characteristics; at high frequency, L_R and C_R are dominant so the transmission-line circuit shows right-handed characteristics. The propagation constant of the resulting structure is given by [16]:

$$\gamma = \alpha + j\beta = \sqrt{ZY} \quad (1)$$

With
$$\beta(\omega) = s(\omega)\sqrt{\omega^2 L_R C_R + \frac{1}{\omega^2 L_L C_L} - \left(\frac{L_R}{L_L} + \frac{C_R}{C_L}\right)} \quad (2)$$

Where
$$s(\omega) = \begin{cases} -1 & \text{if} \quad \omega < \omega_{se} = \min\left(\frac{1}{\sqrt{L_R C_L}}, \frac{1}{\sqrt{L_L C_R}}\right) \\ 0 & \text{if} \quad \omega_{se} < \omega < \omega_{sh} \\ +1 & \text{if} \quad \omega > \omega_{sh} = \max\left(\frac{1}{\sqrt{L_R C_L}}, \frac{1}{\sqrt{L_L C_R}}\right) \end{cases} \quad (3)$$

and
$$Z(\omega) = j\left(\omega L_R - \frac{1}{\omega C_L}\right) \quad (4)$$

$$Y(\omega) = j\left(\omega C_R - \frac{1}{\omega L_L}\right) \quad (5)$$

Parameters $\beta(\omega)$, $s(\omega)$, $Z(\omega)$ and $Y(\omega)$ are a function of frequency and represent dispersion, sign function, impedance and admittance of the antenna structure, respectively. Also, the series and shunt resonance frequencies are, respectively:

$$\omega_{se} = \frac{1}{\sqrt{L_R C_L}} \quad (6)$$

$$\omega_{sh} = \frac{1}{\sqrt{L_L C_R}} \quad (7)$$

Also, the phase and group velocities are defined as:

$$v_p = \frac{\omega}{\beta} = \omega^2\sqrt{L_L C_L} \quad (8)$$

$$v_g = \left(\frac{\partial\beta}{\partial\omega}\right)^{-1} = \omega^2\sqrt{L_L C_L} \quad (9)$$

The antenna's dispersion diagram in Fig. 10(f) shows the bandwidth of structure changes from high-pass left-handed response with cut-off frequency ω_L to low-pass right-handed response with cut-off frequency ω_R with no obvious stop-band. The cut-off frequencies ω_L and ω_R are given below,

$$\omega_L = \frac{1}{\sqrt{L_L C_L}} \quad (10)$$

$$\omega_R = \frac{1}{\sqrt{L_R C_R}}. \quad (11)$$

Table 1: Structural parameters of the proposed antenna and meandered strip-line feed.

Dimensions (mm)

L	W	W_p	L_p	L_g	L_{s1}	L_{s2}	W_{s1}	W_{s2}	W_{s3}
21.2	15	12.7	13.5	3.6	12	8.5	2.4	2.4	0.6

W_{s4}	W_{s5}	W_{s6}	L_1	L_m	L_{m1}	L_{m2}	L_{m3}	W_{m1}	W_m
0.6	1.2	1.2	3.5	4.5	0.9	0.9	0.3	0.3	1.2

Components (pF, nH, Ω, S)

$C_{L,H}$	$C_{L,Inv.U,Left}$	$C_{L,Inv.U,Right}$	C_R	L_L	L_R	R_L	R_R	G_L	G_R
4.5	3.1	3.1	2	5.1	2.3	1.6	0.8	1.3	0.5

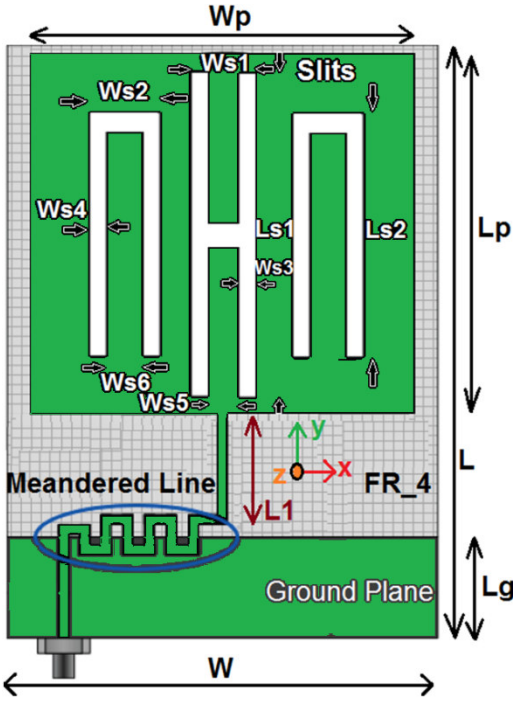

(a)

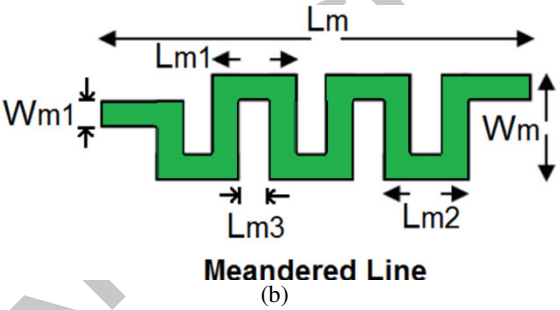

(b)

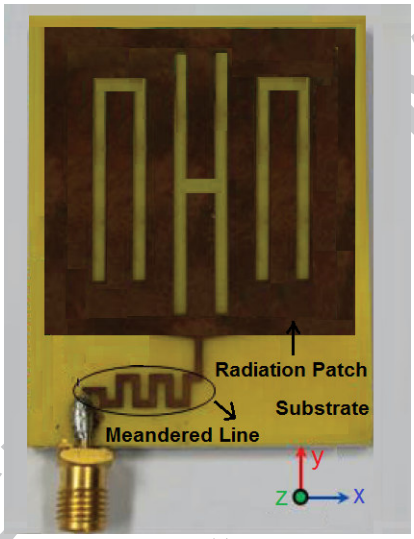

(c)

(d)

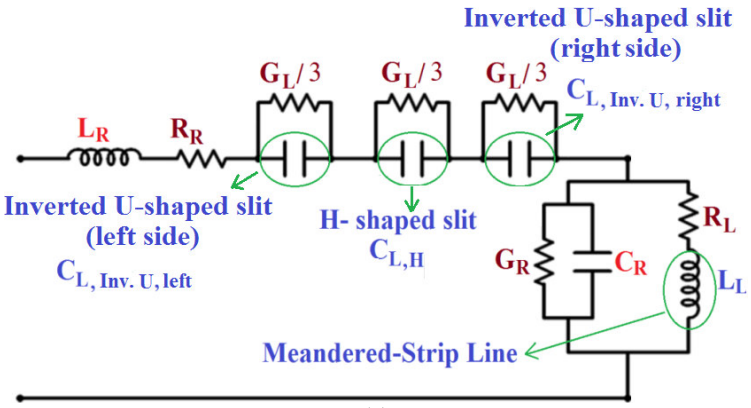

(e)

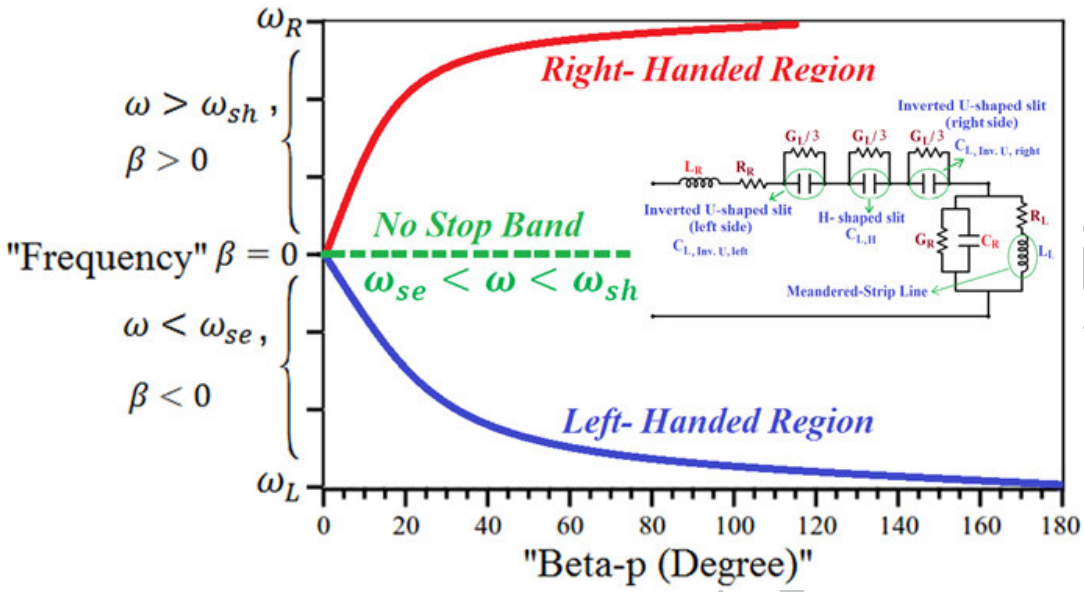

(f)

Fig. 10. (a) Simulation layout of Antenna#4, (b) meandered strip-line layout, (c) fabricated prototype of Antenna#4, (d) antenna ground-plane, (e) equivalent circuit model, and (f) dispersion diagram.

Fig. 11(a) shows Antenna#4 generates three resonance responses at 2.05, 3.7 and 4.45 GHz, each one corresponding to the individual slits embedded in the antenna. The first resonance is due to the inverted U-slit on the left-hand side of the H-slit, the second resonance is due to the H-slit, and the third resonance results from the inverted U-slit on the right-hand side of the H-slit. The simulated and measured impedance bandwidths of Antenna#4 are 5.55 GHz (0.65–6.2 GHz) and 5.25 GHz (0.8–6.05 GHz), respectively, and the corresponding fractional bandwidths are 162.04% and 153.28%, respectively. Antenna#4 operates across band the following communications standards: UHF RFID, WLAN, WiMAX, WiFi, Bluetooth, GPS, PCS, and DCS. Electrical size of the antenna in terms of free-space wavelength at 800 MHz is $0.056\lambda_0 \times 0.040\lambda_0 \times 0.002\lambda_0$, making it suitable for integration in portable microwave devices.

The measured gain and radiation efficiency of Antenna#4 in Fig. 11(b) at 0.8, 2.05, 3.7, 4.45 and 6.05 GHz are 0.95 dBi and 25.75%, 3.85 dBi and 63.12 %, 4.73 dBi and 75.90%, 5.35 dBi and 84.12%, and 3.05 dBi and 50.20%, respectively. The antenna exhibits an optimum gain and radiation efficiency of 5.35 dBi and 84.12% at 4.45 GHz. The measured radiation patterns of Antenna#4 at its resonance frequencies are shown in Fig. 11(c). The radiation field in the E-plane is omni-directional. In the H-plane the antenna radiates bi-directionally across its operational bandwidth.

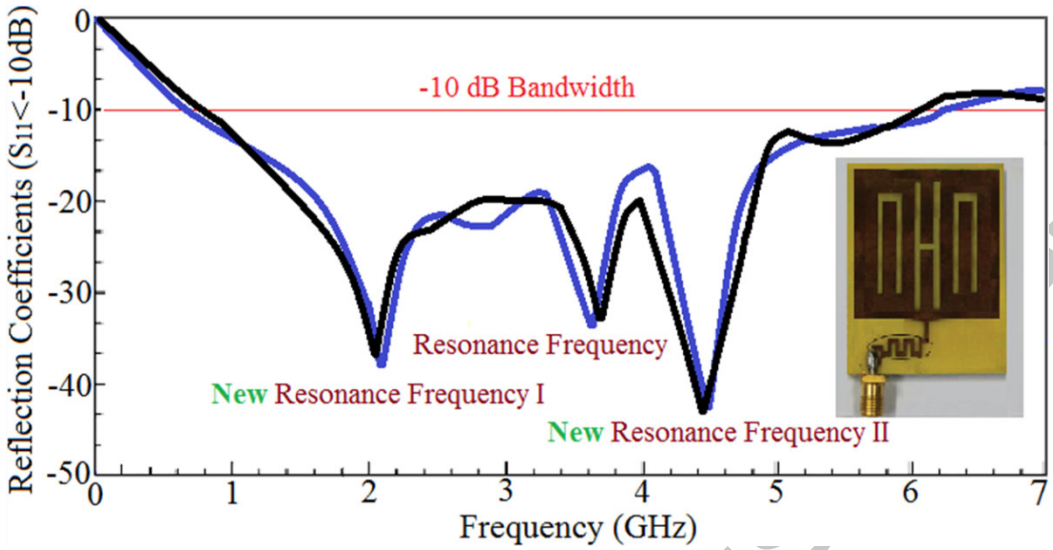

Fig. 11. (a) Simulated (blue line) and measured (black line) reflection-coefficient response of Antenna#4.

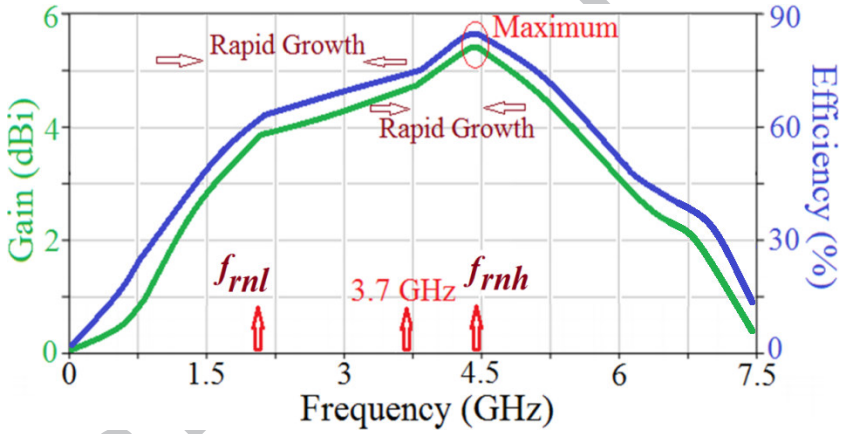

Fig. 11. (b) Measured gain and radiation efficiency of Antenna#4.

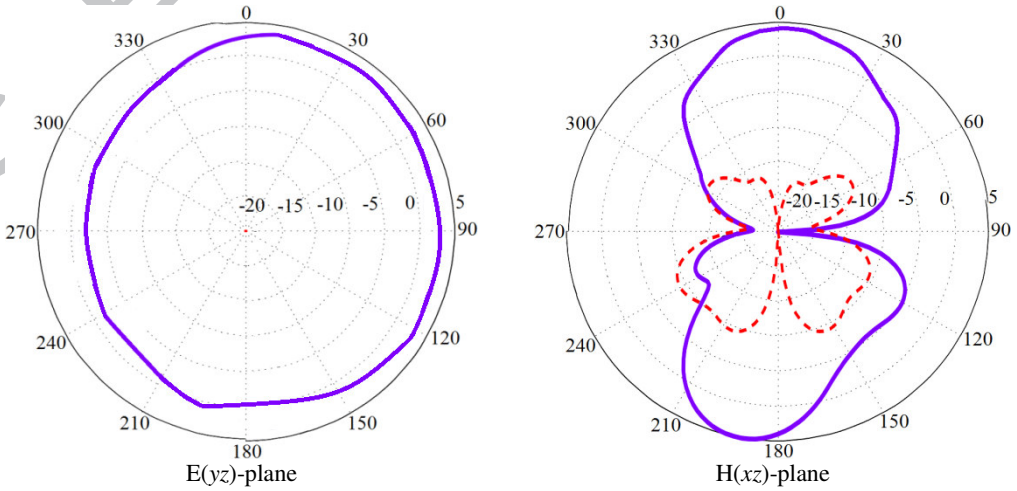

At f_{r1} =2.05 GHz, due to the left-hand side inverted U-slit

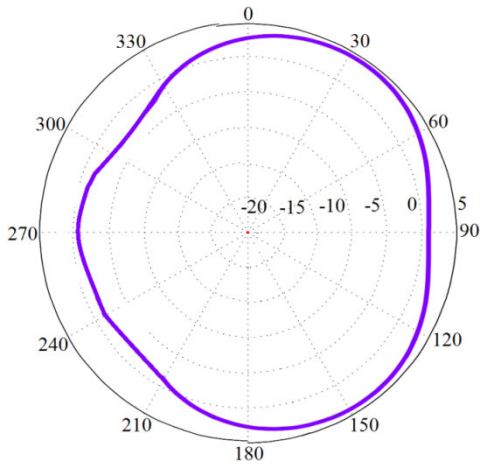

E(*yz*)-plane

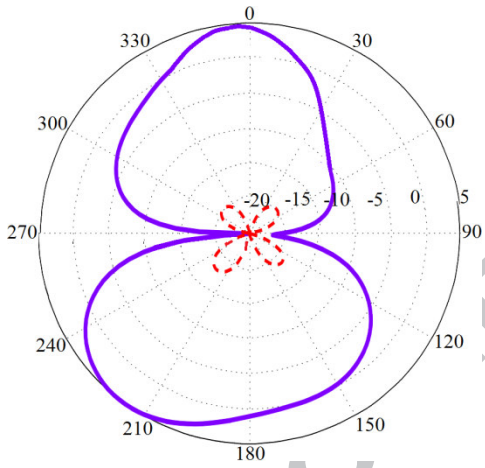

H(*xz*)-plane

At f_{r2} =3.7 GHz, due to the middle H-slit

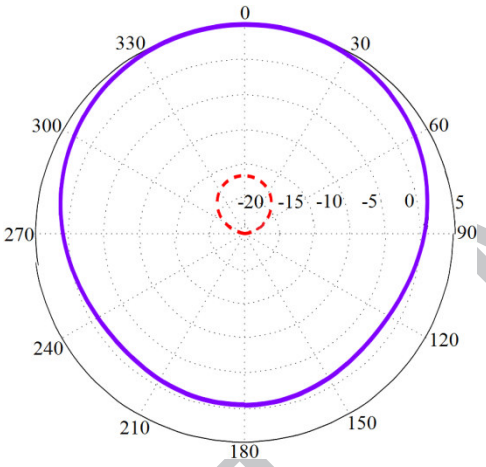

E(*yz*)-plane

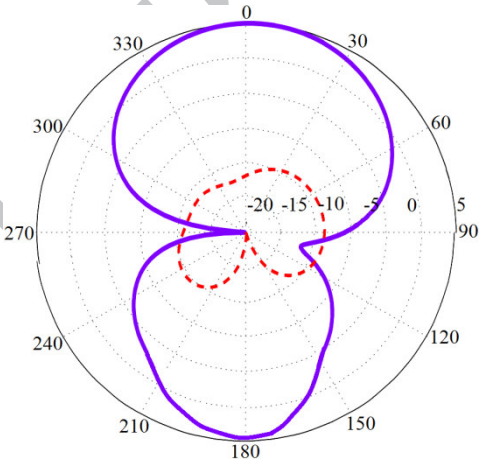

H(*xz*)-plane

At f_{r3} = 4.45 GHz, due to the right-hand side inverted U-slit

Fig. 11. (c) Measured radiation patterns of Antenna#4 at 2.05, 3.7 and 4.45 GHz. Left column: E (*yz*)-plane pattern; Right column: H (*xz*)-plane pattern. [Solid line: co-polarizations, and dashed line: cross polarizations]. Note: in some E-plane patterns the cross-polarization is not visible as it is well below -30 dB.

III. PARAMETRIC STUDY

In order to understand the effect of the slits and the meandered strip-line feed on the performance of Antenna#4 it was necessary to conduct a parametric study. Fig. 12(a) shows that by increasing the length (L_{S1}) and width (W_{S3}) of H-shaped slit significantly improves the impedance bandwidth and the impedance matching of the antenna. The results are tabulated in Table 2. All other structural parameters given in Table 1 remained fixed.

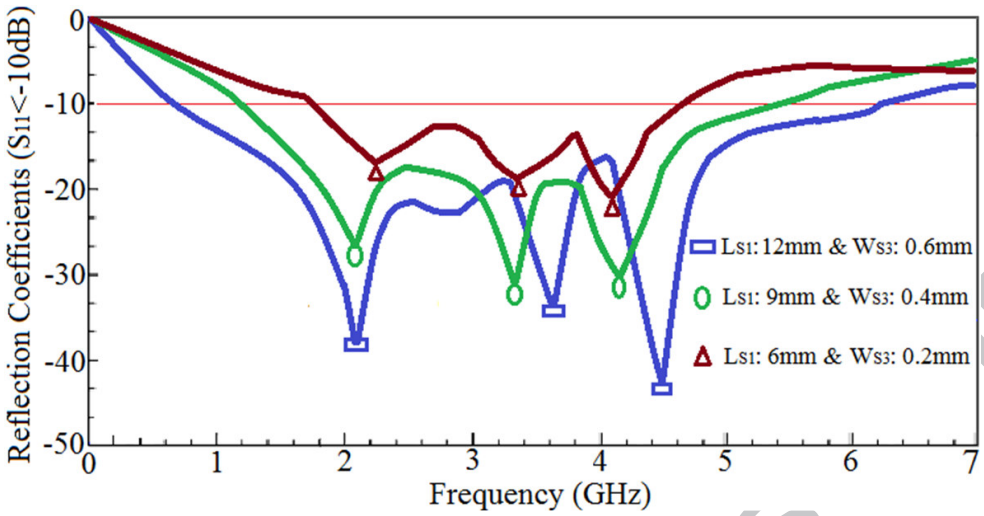

Fig. 12. (a) The effect on the antenna impedance bandwidth as a function of H-slit length (L_{S1}) and width (W_{S3}). All other structural parameters given in Table 1 remain fixed.

Table 2. Effect of various lengths and widths of H-shaped slit on the antenna bandwidth.

Length and Width (mm)	*Frequency Bandwidth (Fractional Bandwidth)*
$L_{S1} = 6$ & $W_{S3} = 0.2$	1.75–4.63 GHz (90.28%) for S_{11} is better than –20 dB
	$f_{r1} = 2.25$ GHz, $f_{r2} = 3.38$ GHz and $f_{r3} = 4.1$ GHz
$L_{S1} = 9$ & $W_{S3} = 0.4$	1.2–5.47 GHz (128.03%) for S_{11} is better than –30 dB
	$f_{r1} = 2.1$ GHz, $f_{r2} = 3.35$ GHz and $f_{r3} = 4.15$ GHz
$L_{S1} = 12$ & $W_{S3} = 0.6$	0.65–6.2 GHz (162.04%) for S_{11} is better than –40 dB
	$f_{r1} = 2.1$ GHz, $f_{r2} = 3.65$ GHz and $f_{r3} = 4.5$ GHz

The effect of inverted U-shaped slit's length (L_{S2}) and width (W_{S4}) on the antenna is shown in Fig. 12(b). This figure shows that by increasing L_{S2} and W_{S4} of the two inverted U-shaped slits the impedance bandwidth and impedance match of the antenna are improved significantly. The results of this analysis are given in Table 3.

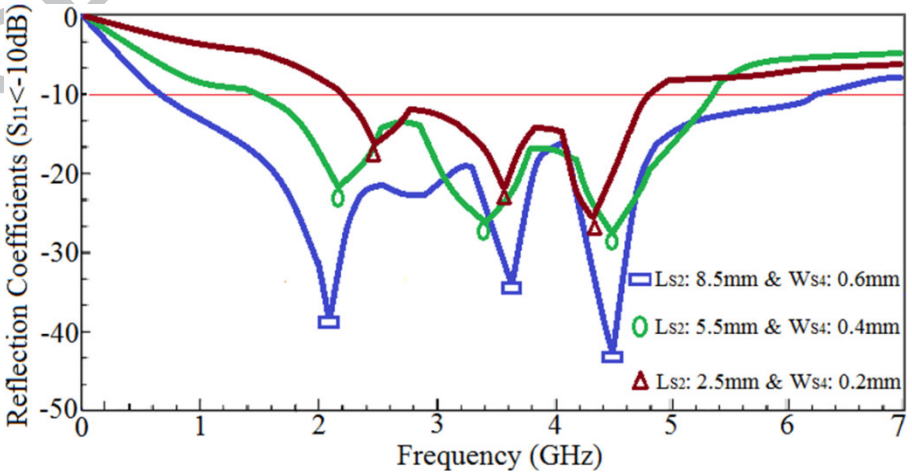

Fig. 12. (b) Parametric study on the antenna as a function of length (L_{S2}) and width (W_{S4}) of the inverted U-shaped slits. All other structural parameters in Table 1 remain fixed.

Table 3. Effect of various lengths and widths of the inverted U-shaped slits on the antenna bandwidth.

Length and Width (mm)	*Frequency Range (Fractional Bandwidth)*
$L_{S2} = 2.5$ & $W_{S4} = 0.2$	2.2 – 4.8 GHz (74.28%) for S_{11} is better than –20 dB
	$f_{r1} = 2.48$, $f_{r2} = 3.58$ and $f_{r3} = 4.34$ GHz
$L_{S2} = 5.5$ & $W_{S4} = 0.4$	1.46 – 5.37 GHz (114.49%) for S_{11} is better than –30 dB
	$f_{r1} = 2.2$, $f_{r2} = 3.2$ and $f_{r3} = 4.48$ GHz
$L_{S2} = 8.5$ & $W_{S4} = 0.6$	0.65 – 6.2 GHz (162.04%) for S_{11} is better than –40 dB
	$f_{r1} = 2.1$, $f_{r2} = 3.65$ and $f_{r3} = 4.5$ GHz

The effect on the antenna performance by the meandered strip-line feed in Fig. 12(c) show it greatly contributes towards improving its impedance match. In fact by increasing the length of L_m, L_{m1} and L_{m2}, and width W_m has virtually no effect on the impedance bandwidth of the antenna, however it significantly improves the antenna's impedance match. Details of these results are provided in Table 4.

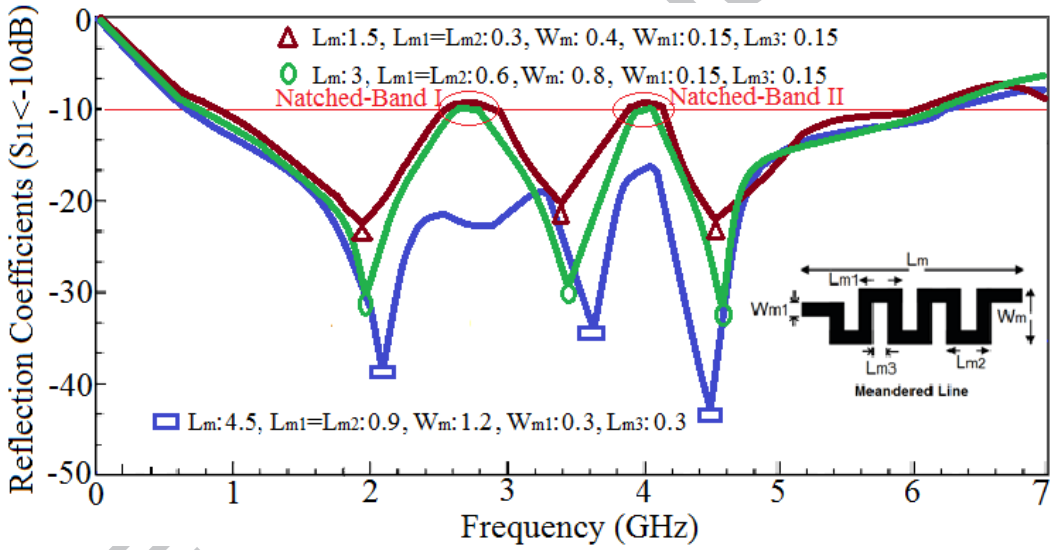

Fig. 12. (c) Antenna impedance bandwidth as a function of meandered strip-line size. All other structural parameters given in Table 1 remain fixed.

Table 4. Results of optimizing the meandered strip-line feed. (Dimensions are in mm)

L_m	L_{m1} & L_{m2}	W_m	W_{m1}	L_{m3}	Notched Band Range
1.5	0.3	0.4	0.15	0.15	I: 2.55 – 2.95 GHz II: 3.85 – 4.15 GHz Impedance match better than –20 dB
3	0.6	0.8	0.15	0.15	I: 2.6 – 2.8 GHz II: 3.95 – 4.05 GHz Impedance matching better than –30 dB
4.5	0.9	1.2	0.3	0.3	Eliminated Impedance matching better than –40 dB

IV. CONCLUSIONS

A simple and effective technique has been demonstrated to extend the impedance bandwidth of patch antennas. This involves embedding three slits in the radiating patch and exciting the antenna through a meandering strip-line. Two inverted U-shape slits are located on either side of the central H-shape slit that are etched on the radiating surface. The antenna structure essentially behaves as a composite left/right-hand metamaterial transmission-line. The proposed technique doesn't affect the dimensions of the radiating patch. The antenna with dimensions of $21.2\times15\times0.8$ mm^3 ($0.056\lambda_0\times0.040\lambda_0\times0.002\lambda_0$ in terms of free-space wavelength at 800 MHz) is shown to provide a fractional bandwidth of 153.28% with 223.27% improvement, a maximum gain of 5.35 dBi and radiation efficiency of 84.12% at 4.45 GHz. Its radiation characteristics are similar to a monopole antenna. The proposed antenna should provide reliable wireless communication across UHF, L, S and C-bands.

REFERENCES

[1] C.Y.D. Sim, F.R. Cai, Y.P. Hsieh, "Multiband slot-ring antenna with single-and dual-capacitive coupled patch for wireless local area network/worldwide interoperability for microwave access operation," IET Microwaves Antennas Propag. Lett., vol. 5, no. 15, pp. 1830-1835, 2011.

[2] J. William, R. Nakkeeran, "A new UWB slot antenna with rejection of WiMax and WLAN bands," Appl. Comp. Electro. Society (ACES) J., vol. 25, no. 9, pp. 787-793, 2010.

[3] S. Noghanian, M.K. Jung, "Ultra wide band planar slot antenna," J. Electromagn. Waves Appl., vol. 22, no. 8-9, pp. 1299-1308, 2008.

[4] M. Alibakhshi-Kenari, M. Naser-Moghadasi, R.A. Sadeghzadah, "The resonating MTM based miniaturized antennas for wide-band RF-microwave systems," Microwave and Optical Technology Letters, vol. 57, pp. 2339–2344, October 2015.

[5] H.-W. Liu, C.-H. Ku, C.F. Yang, "Novel CPW-fed planar monopole antenna for WiMAX/WLAN applications," IEEE Antennas Wirel. Propag. Lett., vol. 9, pp. 240-243, 2010.

[6] X.-L. Ma, W. Shao, G.-Q. He, "A novel dual narrow band-notched CPW-Fed UWB slot antenna with parasitic strips," Appl. Comp. Electro. Society (ACES) J., vol. 27, no. 7, pp. 581-586, 2012.

[7] M.S. Rabbani, H. Ghafouri-Shiraz, "Simple methods for enhancing bandwidth of a rectangular microstrip patch antenna," IET Annual Active and Passive RF Devices Seminar, pp.1-4, 2014.

[8] A. Pirhadi, H. Bahrami, A. Mallahzadeh, "Electromagnetic band gap (EBG) superstrate resonator antenna design for monopulse radiation pattern," Appl. Comp. Electro. Society (ACES) J., vol. 27, no. 11, pp. 908-917, 2012.

[9] K.L. Chung, S. Chaimool, "Broadside gain and bandwidth enhancement of microstrip patch antenna using a MNZ-metasurface," Microw. Opt. Technol. Lett., vol. 54, no. 2, pp. 529-532, 2012.

[10] M. Palandöken, Artificial Materials based Microstrip Antenna Design, Chapter 3, Microstrip Antennas, InTech 2011. ISBN 978-953-307-247-0

[11] M. Alibakhshi-Kenari, M. Naser-Moghadasi, B.S. Virdee, A. Andújar, J. Anguera, "Compact antenna based on a composite right/left handed transmission line," Microwave and Optical Technology Letters, vol.57, issue 8, pp. 1785–1788, August 2015.

[12] H.-W. Lai, K.-M. Luk, "Wideband patch antenna fed by printed meandering strip," Microw. Opt. Technol. Lett., vol. 50, no. 1, pp. 188-192, 2008.

[13] Z. Wang, S. Fang, S. Fu, and S. Jia, "Single-fed broadband circularly polarized stacked patch antenna with horizontally meandered strip for universal UHF RFID applications," IEEE Trans. Microw. Theory Tech., vol. 59, no. 4, pp. 1066-1073, 2011.

[14] P. Wang, G.-J. Wen, Y.-J. Huang, Y.-H. Sun, "Compact CPW-fed planar monopole antenna with distinct triple bands for WiFi/WiMAX applications," Electron. Lett., vol. 48, no. 7, pp. 357-359, 2012.

[15] ANSYS® High Frequency Structural Simulator (HFSS). ANSYS, Inc., USA.

[16] C. Caloz, T. Itoh, Electromagnetic Metamaterials: Transmission Line Theory and Microwave Applications, Wiley-IEEE Press, Dec. 2005. ISBN: 978-0-471-66985-2.

Mohammad Alibakhshi-Kenari was born in Freydonkenar, Iran on February 1988. He received the B.Sc. (Feb. 2010) and M.Sc. (Feb. 2013) degrees in Electrical Engineering and Telecommunication from the Islamic Azad University, Najafabad Branch of Esfahan, Iran and Shahid Bahonar University of Kerman, Iran, respectively. His research interests include microwave and millimeter-wave circuits, transceivers, antennas and wave-propagation, CRLH-TLs, metamaterials, integrated RF-technologies, embedded systems, electromagnetic-waves applications and wireless telecommunication systems. He is now "Editor-in-Chief" in Journal Club for Electronic and Communication Engineering and member of the Applied Computational Electromagnetics Society (ACES). He also is a reviewer for several journals including IEEE TIE, IET MAP, IEEE PTL, OSA, Wiley, Elsevier, Taylor & Francis, Springer and ACES. Mr. Alibakhshi has served as a Member of the Technical Program Committee (M-TPC) at IEEE international conferences. To date he has been published several journal papers.

Mohammad Naser-Moghadasi was born in Iran, in 1959. He received the B.Sc. degree in Communication Eng. in 1985 from the Leeds Metropolitan University (formerly Leeds Polytechnic)-UK. Between 1985-1987 he worked as an RF-design-engineer for the Gigatech company in Newcastle Upon Tyne-UK. From 1987-1989, he was awarded a full scholarship by the Leeds Educational Authority to pursue an M.Phil. on Studying CAD of microwave-circuits. He received his Ph.D. in 1993, from the University of Bradford-UK. He was offered then a two-years post-doc. at the University of Nottingham-UK, to pursue research on microwave cooking of materials. From 1995, Dr. Naser-Moghadasi joined Islamic Azad University, Science and Research Branch, Iran-Tehran, where he currently is head of postgraduate studies. His main areas of interest in research are microstrip antenna, microwave passive and active circuits, RF MEMS. Dr. Naser-Moghadasi is member of the IET, MIET and IEICE. He has so far published over 150 papers.

Ramazan Ali Sadeghzadeh received his B.Sc. in1984 in Telecommunicationn Engineering from the Khajeh Nassir Toosi, University of Technology, Tehran-Iran, and M.Sc. in digital Communications Engineering from the University of Bradford and UMIST (University of Manchester, Institute of Science and Technology)-UK, as a joint program in 1987. He received his Ph.D. in electromagnetic and antenna from the University of Bradford-UK, in 1990. He worked as a Post-Doctoral Research assistant in the field of propagation, electromagnetic, antenna, Bio-Medical, and Wireless communications from 1990 till 1997. From 1984 to 1985 he was with Telecommunication Company of Iran (TCI) working on Networking. Since 1997 he is with K.N. Toosi University of Technology working with Telecommunications Dept. at faculty of Electrical and Computer Engineering. He has published more than 75 referable papers in international journals and conferences. Dr. Sadeghzadeh's current interests are numerical techniques in electromagnetic, antenna, propagation, radio networks, wireless communications, nano-antennas, and radar-systems.

Bal Singh Virdee received the B.Sc. and MPhil degrees in Communications-Engineering from the University of Leeds-UK and his Ph.D. in Electronic-Engineering from the University of London-UK. He has worked in industry for various companies including Philips (UK) as an R&D-engineer and Filtronic-Components Ltd. as a future products developer in the area of RF/microwave communications. He has taught at several academic institutions before joining London Metropolitan University where he is a Professor of Microwave-Communications in the Faculty of Life Sciences&Computing where he Heads the Center for Communications-Technology and is the Director of London Metropolitan-Microwaves. His research, in collaboration with industry and academia, is in the area of

microwave wireless communications encompassing mobile-phones to satellite-technology. Prof. Virdee has chaired technical sessions at IEEE international conferences and published numerous research-papers. He is Executive-Member of IET's Technical and Professional Network Committee on RF/Microwave-Technology. He is a Fellow of IET and a Senior-Member of IEEE.

Ernesto Limiti is a full professor of Electronics in the Engineering Faculty of the University of Roma Tor Vergata since 2002, after being research and teaching assistant (since 1991) and associate professor (since 1998) in the same University. His research activity is focused on three main lines, all of them belonging to the microwave and millimetre-wave electronics area. The first one is related to characterisation and modelling for active and passive microwave and millimetre-wave devices. Regarding active devices, the research line is oriented to the small-signal, noise and large signal modelling as well as devices on diamond substrates. Novel methodologies have been developed and equivalent-circuit modelling strategies have been implemented both for small and large-signal operating regimes for different device technologies. Design methodologies and characterisation methods for low noise devices and circuits are also in focus, as well as the analysis and design methodologies for linear and nonlinear microwave circuits. The above research lines have produced more than 300 publications on refereed international journals and presentations within international conferences. Ernesto Limiti acts as a referee of international journals of the microwave and millimetre wave electronics sector and he is in the steering committee of international conferences and workshops.